

Original Article

A new approach to predict the post-impact fatigue life of prosthetic feet

Haipo Cui^{1,2}, Shuangqing Wang¹, Chengli Song¹

¹Shanghai Institute for Minimally Invasive Therapy, University of Shanghai for Science and Technology, Shanghai 200093, P. R. China; ²Jiangsu Province Key Laboratory of Aerospace Power Systems, Nanjing University of Aeronautics and Astronautics, Nanjing 210016, P. R. China

Received July 15, 2017; Accepted August 7, 2017; Epub October 15, 2017; Published October 30, 2017

Abstract: *Objective:* Prosthetic limb is an important tool for the patients with physical disabilities. An analytical method was proposed for the optimum design of prosthetic feet made of carbon-fiber-reinforced composites. *Method:* A whole-process analysis approach was presented to analyze the process of impact damage initiation and damage development in prosthetic feet, with subsequent fatigue loading analysis. The real impact damage status of prosthetic feet was used to analyze the fatigue characteristics, eliminating the assumptions required by traditional methods. *Results:* A comparison of fatigue life from numerical simulations and experimental tests showed agreement within 12%. *Conclusions:* The proposed method avoids the need to perform large number of experiments to obtain the impact damage status parameters. A parametric modeling program based on the analytical method has been developed to analyze composite structures with any ply orientation.

Keywords: Failure analysis, impact damage, fatigue life, analytical method

Introduction

For the patients with physical disabilities, prosthetic limb is an important tool for them to return normal life. The weight of a prosthetic limb directly affects the energy required by its user to move, influencing its effectiveness and the comfort of its user. It is therefore desirable that prosthetic limbs is designed and constructed using the lightest materials possible. Carbon-fiber-reinforced composites have become a popular choice of material for prosthetic limb production because they are light, strong, and resistant to fatigue [1]. However, fiber-reinforced composite structures are sensitive to impact loading, and even low-energy impacts can significantly decrease structural fatigue performance, possibly leading to catastrophic failure [2]. To ensure their safe use in prosthetic limbs, it is important to thoroughly understand the mechanisms of impact damage and fatigue in structural components made of carbon-fiber-reinforced composite materials. These subjects have been explored in previous work using a combination of experimental observations and computer simulations [3-5].

Long [6], Shi [7], and Xiao [8] carried out computational analyses to predict post-impact delamination, intra- and interlayer cracking, and impact damage area within laminates. Tarpani [9] performed impact and fatigue experiments on carbon-fiber-reinforced poly-phenylene sulfide laminate coupons. Koo [10] proposed a theoretical model for predicting post-impact fatigue life of woven carbon-fiber-reinforced plastic composite laminates. In this model, the impact-damaged area was replaced with an equivalent hole notch. Zhang [11] prefabricated composite laminates with impacted or quasi-static indented damage using two material systems. Static compression strength and compression-compression fatigue testing were carried out and revealed that, quasi-static indentation could not be considered equivalent to impact damage. Naderi [12] proposed a linear fatigue damage model to predict the residual fatigue strength of post-impact laminates. This model was based on a series of impact and post-impact fatigue experiments on fiber-reinforced composite laminates and, although effective, this model required separate testing to determine the model parameters for each material system.

New approach to predict post-impact fatigue life

Table 1. Material property degradation rules

Damage mode	E_{xx}	E_{yy}	E_{zz}	G_{xy}	G_{yz}	G_{xz}	u_{xy}	u_{yz}	u_{xz}
Fiber crushing	$0.07E_{xx}$	$0.07E_{yy}$	$0.07E_{zz}$	$0.07G_{xy}$	$0.07G_{yz}$	$0.07G_{xz}$	$0.07u_{xy}$	$0.07u_{yz}$	$0.07u_{xz}$
Fiber fracture	$0.14E_{xx}$	$0.14E_{yy}$	$0.14E_{zz}$	$0.14G_{xy}$	$0.14G_{yz}$	$0.14G_{xz}$	$0.14u_{xy}$	$0.14u_{yz}$	$0.14u_{xz}$
Matrix cracking	E_{xx}	$0.2E_{yy}$	E_{zz}	$0.2G_{xy}$	$0.2G_{yz}$	G_{xz}	u_{xy}	u_{yz}	u_{xz}
Matrix crushing	E_{xx}	$0.4E_{yy}$	E_{zz}	$0.4G_{xy}$	$0.4G_{yz}$	G_{xz}	u_{xy}	u_{yz}	u_{xz}
Delamination	E_{xx}	E_{yy}	0	G_{xy}	0	0	u_{xy}	0	0
Fiber-matrix shear-out	E_{xx}	E_{yy}	E_{zz}	0	G_{yz}	G_{xz}	0	u_{yz}	u_{xz}

In the studies discussed above, the impact process is analyzed individually or fatigue properties are predicted based on assumptions about impact damage. These assumptions not only limit the accuracy of fatigue life predictions, but also require extensive and costly testing to determine the correct model parameters. In present study, a whole-process analysis approach for exploring the impact and fatigue damage process was proposed, using the 3D progressive damage theory. This approach includes the analysis of the entire damage initiation and development process of composite structures under impact loading, the fatigue loading after impact, and the prediction of fatigue life. The real impact damage status of composite structures was used in analyzing the fatigue property, eliminating the need for the assumptions required in traditional methods. This integrated approach will improve the accuracy of fatigue life predictions and alleviate the need for large number of experiments to determine the impact damage parameters. Furthermore, by using this approach, the fatigue life can be predicted directly from the impact energy. Based on the analytical method, a parametric modeling program has been developed to predict the impact damage process and fatigue lifetimes of composite structures with any ply orientation.

Materials and methods

Impact damage analysis

Composite structures demonstrate five types of failure mode under impact loading: matrix cracking, matrix crushing, fiber fracture, fiber crushing, and delamination. Hou [13] considered the effect of each type of stress component on each of the failure modes and proposed failure criteria for matrix cracking, matrix crushing, fiber fracture, and delamination. This paper improved upon these criteria as follows:

Matrix cracking ($\sigma_{yy} \geq 0$)

$$\left[\frac{\sigma_{yy}}{Y_T}\right]^2 + \left[\frac{\sigma_{xy}}{S_{xy}}\right]^2 + \left[\frac{\sigma_{yz}}{S_{myz}}\right]^2 \geq 1 \quad (1)$$

Matrix crushing ($\sigma_{yy} < 0$)

$$\frac{1}{4} \left[\frac{-\sigma_{yy}}{S_{xy}}\right]^2 + \frac{Y_C^2 \sigma_{yy}}{4S_{xy}^2 Y_C} - \frac{\sigma_{yy}}{Y_C} + \left[\frac{\sigma_{xy}}{S_{xy}}\right]^2 \geq 1 \quad (2)$$

Fiber fracture ($\sigma_{xx} \geq 0$)

$$\left[\frac{\sigma_{xx}}{X_T}\right]^2 + \left[\frac{\sigma_{xy}^2}{S_f^2}\right] + \left[\frac{\sigma_{xz}^2}{S_f^2}\right] \geq 1 \quad (3)$$

Fiber crushing ($\sigma_{xx} < 0$)

$$\left[\frac{\sigma_{xx}}{X_C}\right]^2 + \left[\frac{\sigma_{xy}^2}{S_f^2}\right] + \left[\frac{\sigma_{xz}^2}{S_f^2}\right] \geq 1 \quad (4)$$

Delamination ($\sigma_{zz} \geq 0$)

$$\left[\frac{\sigma_{yz}}{S_{yz}}\right]^2 + \left[\frac{\sigma_{xz}}{S_{yz}}\right]^2 + \left[\frac{\sigma_{yy}}{Y_T}\right]^2 + \left[\frac{\sigma_{zz}}{Z_T}\right]^2 \geq 1 \quad (5)$$

where σ_{ij} and S_{ij} are the layer stress and shear strength components, respectively, with reference to a local coordinate system. In this system, the x- and y-axes are parallel and transverse to the fiber direction, respectively, while the z-axis coincides with the normal direction. In the denominators of these criteria, the subscripts *T* and *C* refer to the tensile and compressive strength, respectively, along the axes defined by X, Y or Z. S_f is the ultimate shear strength of the fiber.

The corresponding failure mode occurs at the position in the structure where the stress components satisfy any one of the criteria above. After this, the load capacity of the structure will change. In this work, a decreased material stiffness at the damaged region was used to characterize the changes in load-bearing capacity, as shown in **Table 1**.

Fatigue damage analysis

Composite structures with impact damage will be further damaged under fatigue loading. There are seven types of damage that can occur: matrix cracking, matrix crushing, fiber-matrix shear-out, fiber fracture, fiber crushing, normal tension, and normal compression. The fatigue failure criteria from Tserpes [14] are used to describe these failure modes as follows:

Matrix cracking fatigue failure criterion ($\sigma_{yy} \geq 0$)

$$\left[\frac{\sigma_{yy}}{Y_f(n, \sigma, k)}\right]^2 + \left[\frac{\sigma_{xy}}{S_{xy}(n, \sigma, k)}\right]^2 + \left[\frac{\sigma_{yz}}{S_{yz}(n, \sigma, k)}\right]^2 \geq 1 \quad (6)$$

Matrix crushing fatigue failure criterion ($\sigma_{yy} < 0$)

$$\left[\frac{\sigma_{yy}}{Y_c(n, \sigma, k)}\right]^2 + \left[\frac{\sigma_{xy}}{S_{xy}(n, \sigma, k)}\right]^2 + \left[\frac{\sigma_{yz}}{S_{yz}(n, \sigma, k)}\right]^2 \geq 1 \quad (7)$$

Fiber-matrix shear-out fatigue failure criterion ($\sigma_{xx} < 0$)

$$\left[\frac{\sigma_{xx}}{X_c(n, \sigma, k)}\right]^2 + \left[\frac{\sigma_{xy}}{S_{xy}(n, \sigma, k)}\right]^2 + \left[\frac{\sigma_{xz}}{S_{xz}(n, \sigma, k)}\right]^2 \geq 1 \quad (8)$$

Fiber fracture fatigue failure criterion ($\sigma_{xx} \geq 0$)

$$\left[\frac{\sigma_{xx}}{X_f(n, \sigma, k)}\right]^2 + \left[\frac{\sigma_{xy}}{S_{xy}(n, \sigma, k)}\right]^2 + \left[\frac{\sigma_{xz}}{S_{xz}(n, \sigma, k)}\right]^2 \geq 1 \quad (9)$$

Fiber crushing fatigue failure criterion ($\sigma_{xx} < 0$)

$$\left[\frac{\sigma_{xx}}{X_c(n, \sigma, k)}\right]^2 \geq 1 \quad (10)$$

Normal tension fatigue failure criterion ($\sigma_{zz} \geq 0$)

$$\left[\frac{\sigma_{zz}}{Z_f(n, \sigma, k)}\right]^2 + \left[\frac{\sigma_{xz}}{S_{xz}(n, \sigma, k)}\right]^2 + \left[\frac{\sigma_{yz}}{S_{yz}(n, \sigma, k)}\right]^2 \geq 1 \quad (11)$$

Normal compression fatigue failure criterion ($\sigma_{zz} < 0$)

$$\left[\frac{\sigma_{zz}}{Z_c(n, \sigma, k)}\right]^2 + \left[\frac{\sigma_{xz}}{S_{xz}(n, \sigma, k)}\right]^2 + \left[\frac{\sigma_{yz}}{S_{yz}(n, \sigma, k)}\right]^2 \geq 1 \quad (12)$$

where $X_i(n, \sigma, k)$, $Y_i(n, \sigma, k)$, and $Z_i(n, \sigma, k)$ are the longitudinal, transverse, and normal residual fatigue strength of unidirectional plies under uniaxial fatigue loading conditions, respectively. The subscripts *T* and *C* represent tension and compression, respectively. $S_{xy}(n, \sigma, k)$ is the in-plane shear residual fatigue strength of unidirectional plies under uniaxial shearing fatigue loading. $S_{xz}(n, \sigma, k)$ and $S_{yz}(n, \sigma, k)$ are the out-of-

plane shear residual fatigue strengths of unidirectional plies under uniaxial shearing fatigue loading, n is the number of load cycles, σ is stress, and k is the stress ratio. The corresponding failure mode occurs when any of the resulting stress components satisfies one of the criteria above.

Under fatigue load cycling, the load-bearing capacity of a material will decrease with an increasing number of loading cycles and the occurrence of fatigue damage. In this work, both the gradual and sudden degradation models were used to describe the observed changes in the load-bearing capacity of the material.

(1) Gradual degradation model

Under fatigue loading, the load-bearing properties of the material will gradually decrease as the number of load cycles increases. A gradual degradation model, based on the criteria proposed by Shokrieh [15], is used to describe these changes:

$$R(n, \sigma, k) = \left\{1 - \left[\frac{\log n - \log 0.25}{\log N_f - \log 0.25}\right]^{\beta}\right\}^{1/\alpha} (R_0 - \sigma) + \sigma \quad (13)$$

$$E(n, \sigma, k) = \left\{1 - \left[\frac{\log n - \log 0.25}{\log N_f - \log 0.25}\right]^{\beta}\right\}^{1/\alpha} \left[E_0 - \frac{\sigma}{\varepsilon_f}\right] + \frac{\sigma}{\varepsilon_f} \quad (14)$$

where R_0 and E_0 are the initial strength and stiffness of undamaged material, respectively, ε_f is the average strain to failure, σ is the maximum fatigue stress level, k is the stress ratio, and N_f is the fatigue life of unidirectional plies under a given fatigue loading (fixed σ and k values).

(2) Sudden degradation model

As the number of fatigue loading cycles increases, fatigue damage will accumulate. When cumulative fatigue damage reaches a certain level, the stress in the structure will satisfy the fatigue failure criteria, and the corresponding failure mode will occur. At this time, the load-bearing properties of the material will undergo a rapid change, described here using a sudden degradation model. This model reduces the load-bearing properties of the material according to the type of failure mode that occurs. According to the equivalent damage principle, the decrease in load-bearing properties of the material depends on the failure mode, regardless of the type of load that caused the failure.

New approach to predict post-impact fatigue life

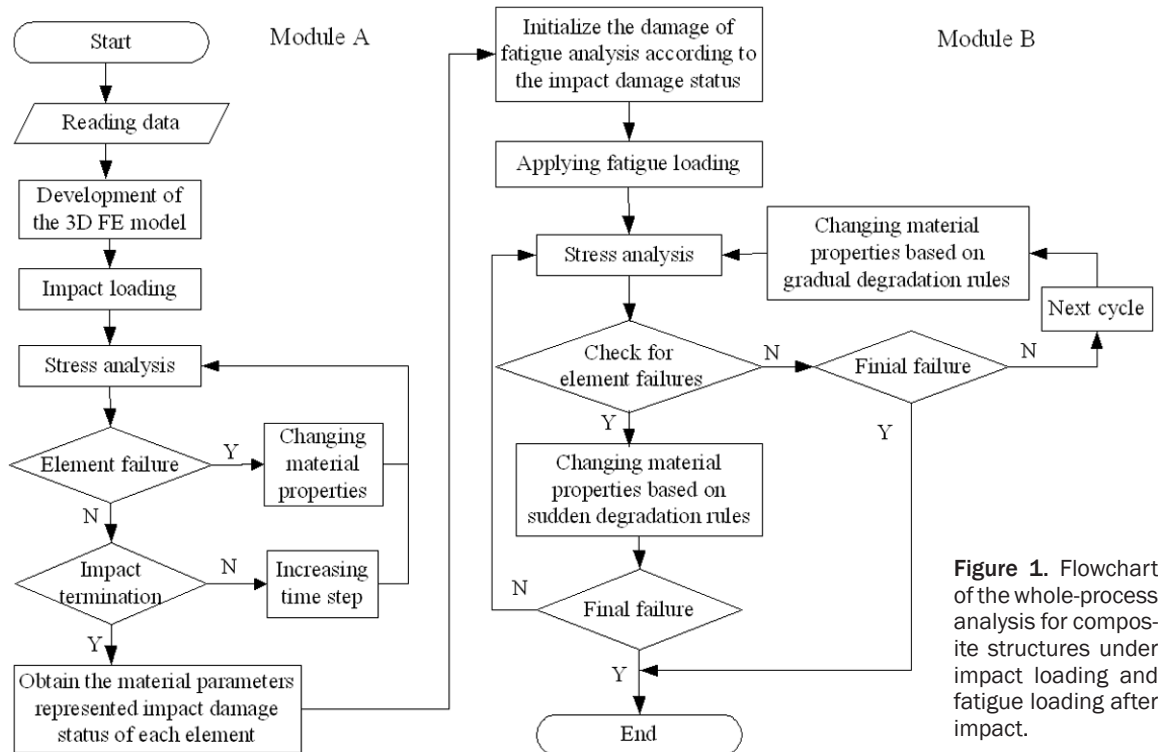


Figure 1. Flowchart of the whole-process analysis for composite structures under impact loading and fatigue loading after impact.

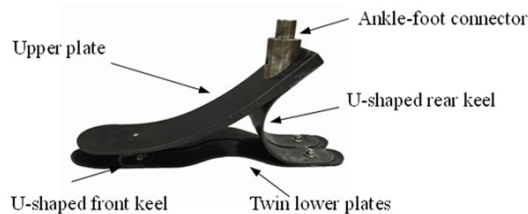


Figure 2. Carbon fiber composite prosthetic foot.

Therefore, the types of degradation rules used here are the same as those in the impact model (Table 1).

Final failure criterion

In addition to determining the failure mode criteria to predict the fatigue life of composite structures following impact damage, it is also necessary to define the criteria for overall structural damage that renders the structure unable to bear further loading. During actual loading processes, when the load-bearing end of the prosthetic rear keel was overloaded, it experienced a sudden large displacement leading to damage of the overall structure. Therefore, it was determined in this study that the displacement of this load bearing end would be compared after every ten load cycles. Structural

failure was defined by a 30% increase in displacement.

Flowchart of the model

Based on the proposed numerical model, a parametric modeling program was developed to predict the impact damage process and fatigue life of composite structures with any ply orientation. The flowchart is shown in Figure 1. Module A represents the flowchart of impact damage analysis, while Module B describes the flowchart of the damage progression and fatigue life prediction of composite structures with impact damage under fatigue loading.

Results

Experimental observations

The structure of the specimens used in the experiments is shown in Figure 2. There are five structural components: the ankle-foot connector, the upper plate, the U-shaped front keel, twin lower plates, and the U-shaped rear keel. Of these components, the one most easily broken by compression-compression fatigue loading is the U-shaped rear keel and is, therefore, the main focus of this work. The thickness of

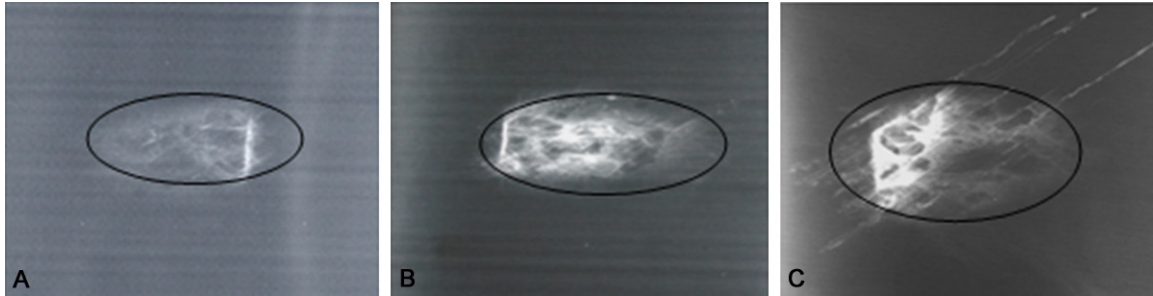


Figure 3. Typical X-radiographs for impact damage. A: 4 J; B: 10 J; C: 16 J.



Figure 4. Fatigue property testing machine for prosthetic foot.

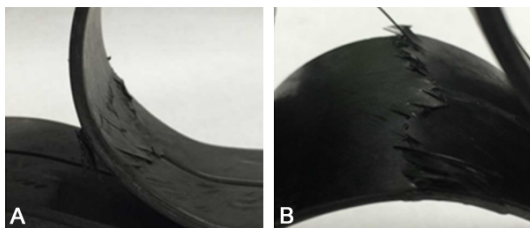


Figure 5. Post-impact fatigue fractures. A: Side view; B: Back view.

the U-shaped rear keel used in these experiments was 2.7 mm and was constructed from T300/BMP-316 composite materials. The sample test configuration was: 45°/-45°/0°/0°/45°/-45°/90°/90°/45°/-45°/90°/90°/45°/-45°/0°/0°/45°/-45°. Impact energies of 4 J, 10 J, and 16 J were selected.

An instrumented drop-weight machine was used to impact the specimens. The center of the U-shaped rear keel was impacted by a 45

Table 2. Material properties of the T300/BMP-316

Elastic parameters		Strength parameters	
$E_{xx'}$ /GPa	128.8	X_T /MPa	1298.2
$E_{yy'}$ /GPa	8.3	X_C /MPa	1269.4
$E_{zz'}$ /GPa	8.3	Y_T /MPa	53.6
G_{xy} /GPa	4.1	Y_C /MPa	185.0
G_{xz} /GPa	4.1	Z_T /MPa	53.6
G_{yz} /GPa	4.1	Z_C /MPa	185.0
u_{xy}	0.355	S_{xy} /MPa	102.0
u_{xz}	0.355	S_{xz} /MPa	102.0
u_{yz}	0.355	S_{yz} /MPa	102.0
		S_f /GPa	193.8

mm diameter hemi-spherical impactor weighing 1.5 kg. The impact energy was varied by changing the velocity of impact rather than the weight. Repeated impacts were avoided when the impactor bounced against the prosthetic foot. **Figure 3** shows typical X-radiographs of the impact damage, with the light color corresponding to damage.

After impact testing, compression-compression fatigue life testing was carried out on each sample. The equipment used is shown in **Figure 4**. The loading frequency was 1.5 Hz and the compressive load was 1280 N. **Figure 5** shows typical fatigue damage in which the fractures intersect the impact-damaged region. In the fracture zone, matrix cracking and fiber fractures are clearly visible. In the side view, delamination damage is visible.

In order to verify the proposed analytical method, numerical results were generated from the model to compare with these experimental data. The material system was T300/BMP-316, and its properties are listed in **Table 2**.

New approach to predict post-impact fatigue life

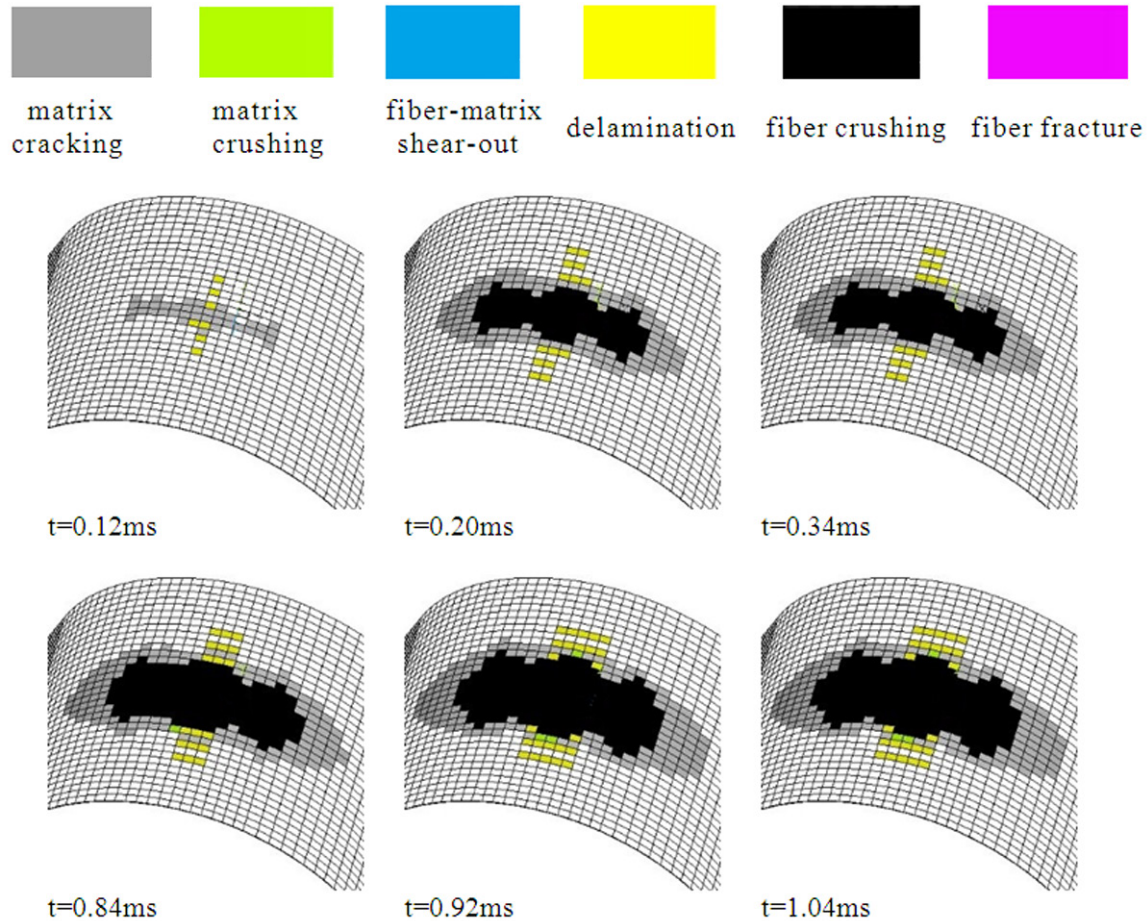


Figure 6. Impact damage at different times.

Impact damage analysis

Figure 6 shows overall damage to the rear keel at different times during impact. The figure demonstrates that initially, damage occurs at the center where the impactor makes contact. Initial damage is mainly matrix cracking and delamination. As time increases, impact damage gradually spreads outward from the point of impact, and fiber crushing occurs over a larger area. Comparing these images at $t=0.92$ ms and $t=1.04$ ms, it can be seen that the type and extent of damage are identical, indicating that by $t=0.92$ ms, the internal stress within each layer had already reached its maximum value, resulting in no further spread of the damage.

Fatigue damage analysis after impact

Following impact analysis, the material parameters representing the damage status of each element can be obtained. According to these parameters, the damage of each element in

the fatigue analysis may be initialized, giving the initial condition for fatigue damage analysis. This process avoids assumptions on the damage status after impact, and demonstrates the whole-process approach to analyzing impact and fatigue damage to the composite prosthetic foot.

After the impact phase is complete, the rear keel is subjected to compression-compression fatigue loading. The compressive load was 1280 N. **Figure 7** shows the damage done to selected layers of the rear keel after the indicated number of fatigue loading cycles. In the figure, the 1st layer is the layer that was struck by the impactor. For brevity, only the analyses of the damage progression in the 1st (45°), 6th (-45°), 8th (90°), 15th (0°), and 18th (-45°) layers of the 18-ply U-shaped rear keel, and only a portion of the rear keel, are displayed. **Figure 7** shows a number of special characteristics of damage propagation during fatigue loading of the rear keel: (1) The inner-most layer (layer 1)

New approach to predict post-impact fatigue life

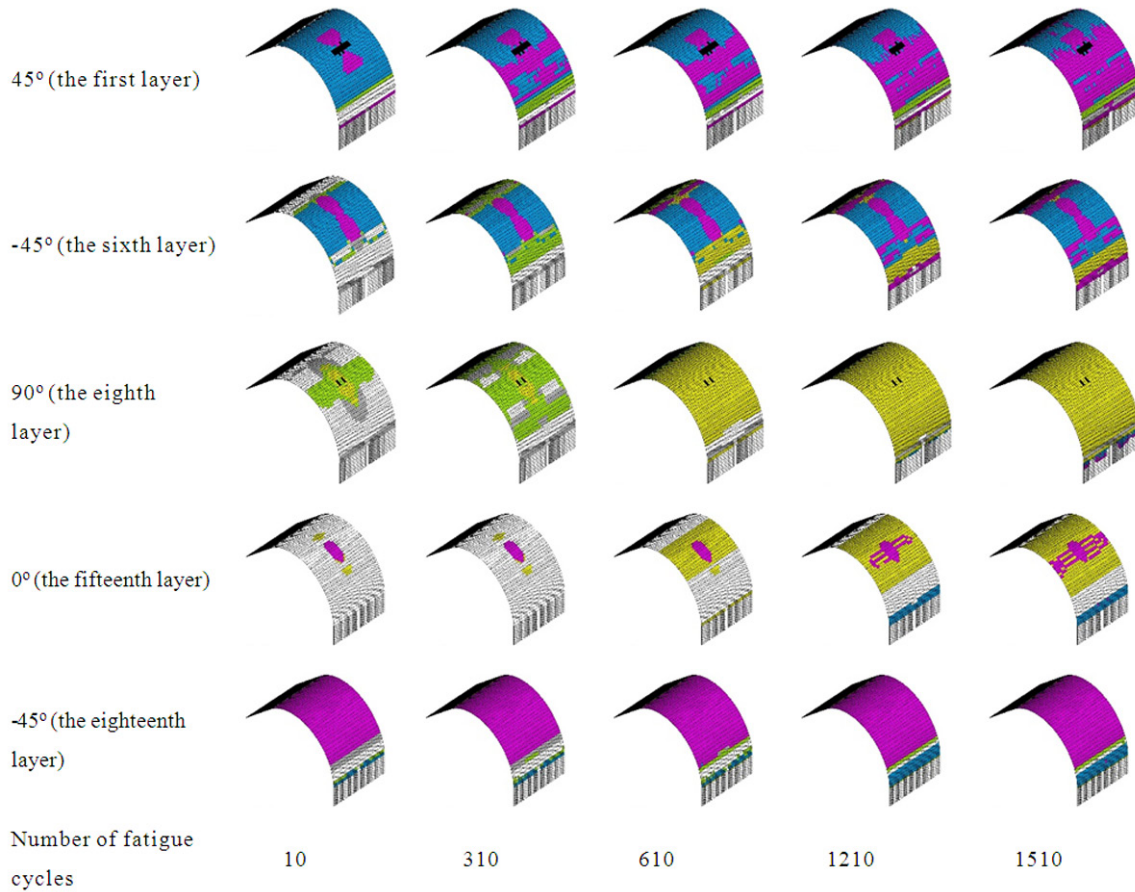


Figure 7. Progressive damage modeling of selected layers under fatigue loading.

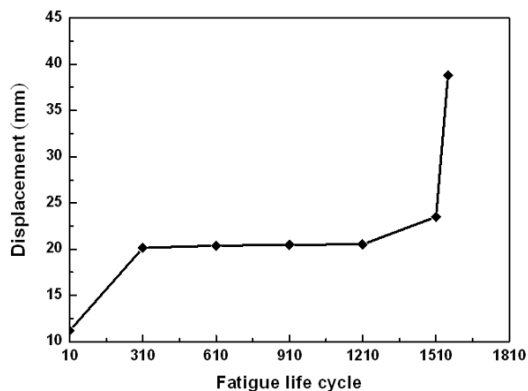


Figure 8. Displacement of loading point versus fatigue life cycle curve.

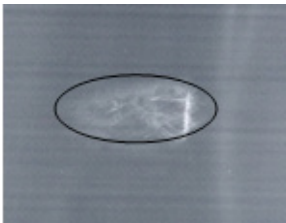
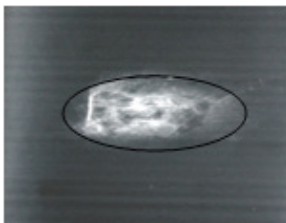
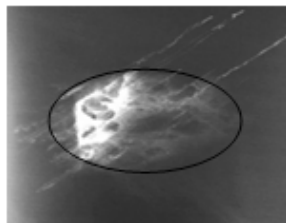
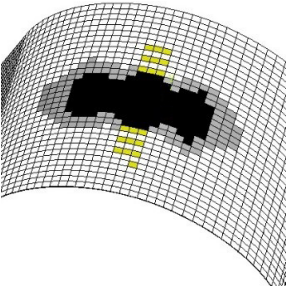
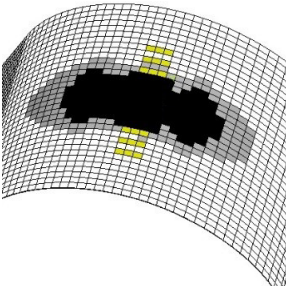
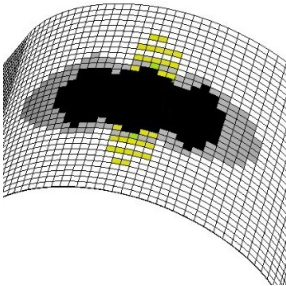
was the first to demonstrate fiber-matrix shear-out, after which fiber fractures occurred. (2) In the outer-most layer (layer 18), fiber fractures were the first type of damage to occur. Extensive fiber fractures occurred in this layer at the onset of fatigue loading. (3) Compared to the $\pm 45^\circ$ ply layers, damage to the 0° ply layer

occurred later. Initially, a few delaminations and fiber fractures appeared at the impact region in the 0° layer. Later, with increasing fatigue cycles, these eventually spread to both sides of the rear keel. (4) Matrix cracking and matrix crushing were the first types of damage to appear in the 90° ply layer and subsequently delamination occurred. However, even following failure of the entire rear keel, there were no fiber fractures in this layer.

Finite element analysis was also used to analyze the displacement of the loading point on the bottom surface of the rear keel as the number of fatigue loading cycles increased. As shown in **Figure 8**, initial changes in the displacement of the loading point were large. Subsequently, loading point displacement remained relatively steady until it suddenly rose again after 1560 loading cycles, indicating that the overall structure had been damaged and the rear keel was no longer able to support fatigue loading. The rear keel of the prosthetic foot, made of carbon-fiber-reinforced compos-

New approach to predict post-impact fatigue life

Table 3. Comparison of predicted and experimental impact damage

Impact energy E/J	4	10	16
Experimental result			
Predicted result			

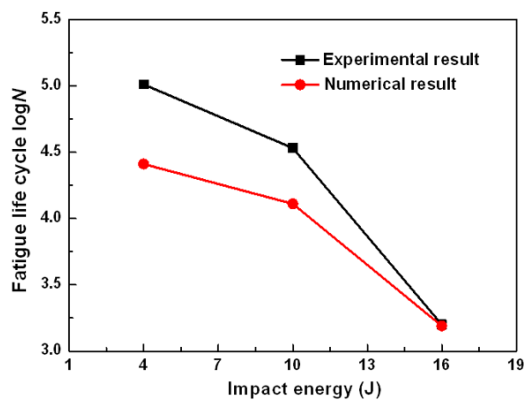


Figure 9. Comparing predicted fatigue life cycles with the experimental results.

Table 4. Predicted and experimental fatigue life results

Impact energy E/J	Experimental result log N	Numerical result log N'	Error (%)
4	5.01	4.41	-11.97
10	4.53	4.11	-9.27
16	3.23	3.19	-1.24

ite, could therefore sustain 1560 compression-compression fatigue loading cycles after a 16 J impact.

Discussion

In this study, a whole-process analysis approach was proposed to analyze the process of impact

damage initiation and damage development in prosthetic feet, with subsequent fatigue loading analysis. **Table 3** shows the experimental and predicted impact damage figures of the prosthetic foot. The table shows that the damaged area gradually increases with impact energy, and the experimental impact damage results are consistent with the model. This demonstrates the validity of the analytical model used in this study and its application in predicting impact damage.

Figure 9 presents a comparison of the predicted and actual post-impact fatigue cycles for each of the three impact energies, with numerical data tabulated in **Table 4**. The cycle numbers in the chart and table are expressed logarithmically. **Figure 9** and **Table 4** exhibit good agreement between the predictions and experimental results. This further demonstrates the validity of the approach developed in this work, including the whole-process analysis method and the theoretical analysis model.

In conclusion, a method for the prediction of low velocity impact damage and fatigue life of composite structures is presented in this work. A whole-process analysis method is proposed to describe the damage initiation and development process of composite structures under impact and post-impact fatigue loading. The real impact damage status of composite structures has been applied to analyze the fatigue life, improving upon the traditional methods

New approach to predict post-impact fatigue life

adopted for analyzing the damage status of composite structures after impact. This not only improves the predictive power and accuracy of the model to estimate fatigue life but also avoids the need to perform a large number of experiments to obtain the impact damage parameters. Furthermore, using this method, the fatigue life after impact can be predicted directly from the impact energy.

Acknowledgements

This project was supported by the National Natural Science Foundation of China (No. 51305268) and Fundamental Research Funds for the Central Universities (No. NJ20160017), P. R. China.

Disclosure of conflict of interest

None.

Address correspondence to: Chengli Song, Shanghai Institute for Minimally Invasive Therapy, University of Shanghai for Science and Technology, 334 Jungong Road, Shanghai 200093, P. R. China. Tel: +86-21-55272107; Fax: +86-21-55270695; E-mail: csong@usst.edu.cn

References

- [1] Pithawa LCA, Singh BG and Ravindranath BG. Clinical appraisal of indigenous below knee endoskeletal carbon fibre prosthesis. *Medical J Armed Forces India* 2006; 62: 108-111.
- [2] Rikard B, Nilsson L and Simonsson K. Simulation of low velocity impact on fiber laminates using a cohesive zone based delamination model. *Compos Sci Technol* 2011; 64: 279-288.
- [3] Schmidt F, Rheinfurth M, Protz R, Horst P, Busse G, Gude M and Hufenbach W. Monitoring of multiaxial fatigue damage evolution in impacted composite tubes using non-destructive evaluation. *Compos Part A-Appl S* 2012; 43: 537-546.
- [4] Koo JM, Choi JH and Seok CS. Prediction of post-impact residual strength and fatigue characteristics after impact of CFRP composite structures. *Compos Part B-Eng* 2014; 61: 300-306.
- [5] Shi WJ, Hu WP, Zhang M and Meng Q. A damage mechanics model for fatigue life prediction of fiber reinforced polymer composite lamina. *Acta Mech Solida Sin* 2011; 24: 399-410.
- [6] Long SC, Yao XH and Zhang XQ. Delamination prediction in composite laminates under low-velocity impact. *Compos Struct* 2015; 132: 290-298.
- [7] Shi Y, Pinna C and Soutis C. Modelling impact damage in composite laminates: a simulation of intra-and inter-laminar cracking. *Compos Struct* 2014; 114: 10-19.
- [8] Xiao SS, Chen PH and Ye Q. Prediction of damage area in laminated composite plates subjected to low velocity impact. *Compos Sci Technol* 2014; 98: 51-56.
- [9] Tarpani JR, Canto RB, Saracura RGM, Ibarra-Castaneda C and Maldague XPV. Compression after impact and fatigue of reconsolidated fiber-reinforced thermoplastic matrix solid composite laminate. *Procedia Mat Sci* 2014; 3: 485-492.
- [10] Koo JM, Choi JH and Seok CS. Evaluation for residual strength and fatigue characteristics after impact in CFRP composites. *Compos Struct* 2013; 105: 58-65.
- [11] Zhang JY, Zhao LB, Li M and Chen YL. Compressive fatigue behavior of low velocity impacted and quasi-static indented CFRP laminates. *Compos Struct* 2015; 133: 1009-1015.
- [12] Naderi S, Hassan MA and Bushroa AR. An empirical modified fatigue damage model for impacted GFRP laminates. *Acta Astronaut* 2014; 103: 119-128.
- [13] Hou JP, Petrinic N, Ruiz C and Hallett SR. Prediction of impact damage in composite plates. *Compos Sci Technol* 2000; 60: 273-281.
- [14] Tserpes KI, Labeas G, Papanikos P and Kermanidis T. Strength prediction of bolted joints in graphite/epoxy composite laminates. *Compos Part B-Eng* 2002; 33: 521-529.
- [15] Shokrieh MM and Lessard LB. Progressive fatigue damage modeling of composite materials, part I: modeling. *J Compos Mater* 2000; 34: 1056-1080.